Journal of Crystal Growth 601 (2023) 126942

Contents lists available at ScienceDirect

Journal of Crystal Growth

journal homepage: www.elsevier.com/locate/jcrysgro

# Effect of melt shearing on D-mannitol crystal twisting in the presence of small molecule and macromolecular additives

Yuze Zhang [a], Alexander G. Shtukenberg [b], Bart Kahr [b], Dilhan M. Kalyon [a], Stephanie S. Lee [a,b,*]

[a] Department of Chemical Engineering and Material Science, Stevens Institute of Technology, Hoboken, NJ 07030, USA
[b] Molecular Design Institute, Department of Chemistry, New York University, New York, NY 10003, USA

ARTICLE INFO

Communicated by James J. De Yoreo

*Keywords:*
A1. Crystal morphology
A1. Melt shearing
A2. Growth from the melt
B1. Organic compounds
B1. Polymers
B1. Twisted Crystals

ABSTRACT

Many molecular crystals grow as twisted lamellae from the melt when the driving force is high, but the mechanisms governing the spontaneous formation of helicoidal crystallites are varied and those operative in particular cases are difficult to identify. Polyvinylpyrrolidone (PVP) induces the crystallization of D-mannitol as banded spherulites comprised of twisted fibrils emanating radially from spherulite nucleation centers. The molecular weight of the PVP phase affects the twisting pitch, $P$, (rotation of the crystallite by 180°), in D-mannitol thin films crystallized from the melt. At a relatively high crystallization temperature ($T_c$ = 130 °C), $P$ was sensitive to the PVP molecular weight, ranging from 390 ± 20 μm for D-mannitol films incorporating 15 wt% 10 kDa PVP to 20 ± 3 μm for the same weight of 1300 kDa PVP. Magnitudes of complex viscosities, $|\eta^*|$, of D-mannitol/PVP melts measured via small-amplitude oscillatory shearing were strongly dependent on the PVP molecular weight, but were not correlated to $P(T)$. Instead, $P$ was sensitive to the dynamic PVP chain conformation during D-mannitol crystallization. Under steady torsional shear, $P$ decreased from ~ 30 μm to ~ 8 μm with increasing shear rates from 0.01 to 100 $s^{-1}$ for D-mannitol films crystallized at 130 °C in the presence of 15 wt% 10 or 1300 kDa PVP. Shear forces decrease the entanglement density of polymer chains while orienting the chains along the stream lines of the viscometric flow, indicating that the conformations of macromolecular additives can affect the pitch of banded spherulites. By contrast, $P$ in D-mannitol twisted by D-sorbitol was independent of shear rate.

## 1. Introduction

The appearance of concentric bands of light transmittance in spherulites between crossed polarizers, mostly associated with polymers but also frequently observed in small molecule crystals,[1] is a tell-tale sign of crystal twisting. Crystalline fibrils grow radially from a nucleation centre, twisting in concert with one another about the growth direction. Concentric bands arise as the anisotropic refractivity precesses with crystal twisting. About 50 % of undercooled homopolymer melts can crystallize as banded spherulites comprising helicoidal lamellae.[2–8] Many small molecules do as well, sometimes when pure [9] and at other times requiring small molecule[1,10] or polymer [11,12] additives. The spacing between concentric bands corresponding to a π rotation about the growth direction, or pitch $P$, can range from microns to millimeters for both small molecules and polymer banded spherulites.

As a product of spontaneous pattern formation with applications in microscale templating,[13–15] chiroptics,[16,17] and optoelectronics, [10,18] banded spherulites have been extensively studied over the past fifty years to understand the mechanisms governing this phenomenon. Considering the diversity of compounds and compositions that can form twisted crystals, it is unlikely that a single mechanism is responsible for this phenomenon across all materials. Entropic pressure introduced by dangling polymer ends at growth fronts,[19] unbalanced surface stresses,[20–23] and autodeformations to relieve internal stress,[24–27] are among several theories to account for growth induced twisting. Hydrodynamic flows at spherulitic growth fronts caused by density differences between the liquid and solid phases are also thought to play a role in crystal twisting in some compounds.[28] This mechanism should depend strongly on the liquid viscosity, and indeed the incorporation of high-viscosity additives, such as natural tree resins or polymers, has been demonstrated to induce crystal twisting in small-molecule crystals. [1] In 2004, Sadlik and Bechhoefer proposed the following scaling law based on hydrodynamic flow-governed crystal twisting:

* Corresponding author.
*E-mail address:* stephlee@nyu.edu (S.S. Lee).

https://doi.org/10.1016/j.jcrysgro.2022.126942
Received 11 June 2022; Received in revised form 7 October 2022; Accepted 14 October 2022
Available online 20 October 2022

$$P \propto \eta^{-\frac{1}{2}} V_s^{-2} \quad (1)$$

where $\eta$ is the viscosity of the liquid phase and $V_s$ is the spherulite growth front velocity.[29] This scaling law accurately predicted the pitch dependence on crystallization temperature for banded spherulites of ethylene carbonate with varying concentrations of 100 kDa polyacrylonitrile but did not match mixtures with 200 kDa polyacrylonitrile.

Here, we examine the role of polymer molecular weight and chain conformations on crystal twisting in small molecule films with a polymer additive (Fig. 1). We previously reported that D-mannitol forms banded spherulites when grown from the melt in the presence of either mannitol's diastereoisomer D-sorbitol or polyvinylpyrrolidone with an average molecular weight of 10 kDa.[30] Pitch in D-mannitol/PVP blends was observed to decrease exponentially with decreasing crystallization temperature. It was also found to depend on the additive concentration, but specific relationships between D-mannitol and PVP remain unclear. Expanding on Sadlik and Bechhoefer's work, here we examine crystal twisting in D-mannitol-PVP blends for PVP molecular weights (MWs) varying from 10 kDa to 1300 kDa. We further introduce shear forces during crystallization, finding that dynamic polymer chain conformations can affect the intensity of D-mannitol crystal twisting. In contrast, the twisting pitch for D-mannitol/D-sorbitol blends was insensitive to shear forces.

## 2. Results and discussion

### 2.1. Crystal twisting pitch dependence on PVP MW

D-Mannitol/PVP blends (85:15 ratio by weight) were crystallized from the melt at temperatures between 50 and 150 °C and for PVP molecular weights of 10, 40, 360, and 1300 kDa (hereafter referred to as PVP10, PVP40, PVP360, and PVP1300). The crystallized samples were cooled to room temperature and imaged with an optical microscope between crossed polarizers. Fig. 2A – D display polarized optical micrographs (POMs) of D-mannitol/PVP films crystallized at 130 °C for the four different PVP molecular weights. For all films, D-mannitol crystallized as banded spherulites in which concentric rings emanating from spherulite centers represent different orientations of crystalline fibrils as they rotate about the growth direction in concert with one another causing a precession in the refractivity. The light and dark bands arise from variance of the retardance and extinction as the crystals rotate around the radial crystallographic axis. An illustration of a twisted fibril overlayed on the bands of a spherulite is displayed in Fig. 2B. The twisting pitch, *P*, defined as the distance between bands, represents a 180° rotation about the growth direction. Scanning electron microscopy and atomic force microscopy characterization of D-mannitol/PVP10 film surfaces previously revealed lamellae with thicknesses ranging from 60 to 180 nm that twist in concert with one another about the spherulitic growth direction.[30] This lamellar morphology is similar to that observed in other small-molecule compounds, including aspirin,[31] hippuric acid,[32] *D* and L-mandelic acid[33] and phthalic acid.[34].

D-Mannitol crystallizes as two polymorphs from the melt, α and δ.[35] Grazing incidence wide-angle X-ray scattering (GIWAXS) patterns

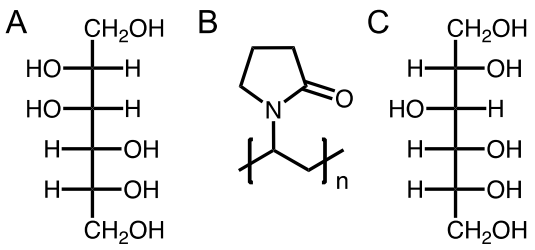


**Fig. 1.** Molecular structures of (A) D-mannitol, (B) PVP, (C) D-sorbitol, respectively.

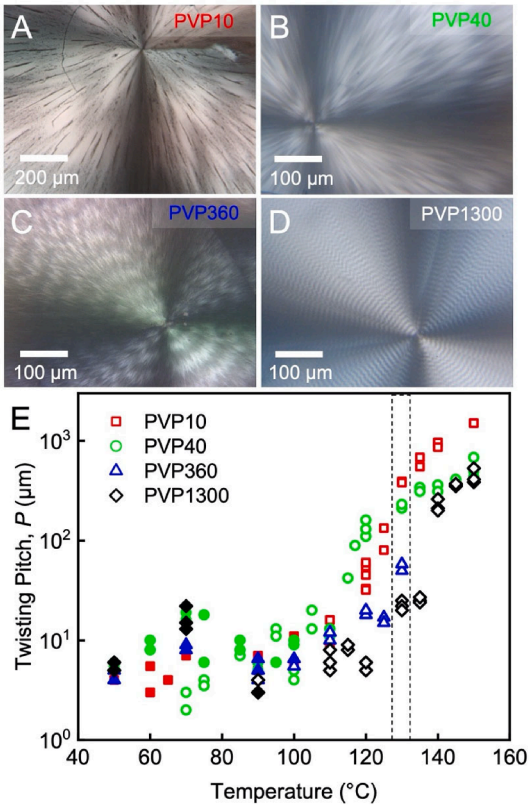


**Fig. 2.** A – D) POMs of D-mannitol films crystallized at 130 °C with 15 wt% of PVP10, PVP40, PVP360 and PVP1300 respectively. E) Twisting pitch dependence of banded spherulites of D-mannitol on the crystallization temperature for D-mannitol films with 15 wt% PVP. The dashed rectangle highlights the region corresponding to the optical micrographs in A – D. Open and filled symbols represent the δ and α polymorph, respectively.

confirmed that D-mannitol crystallizes as the δ polymorph at 130 °C and a PVP concentration of 15 wt% for all PVP MWs tested (Figure S1). With decreasing crystallization temperature, diffraction peaks associated with the α phase were also present (Figure S1). In POMs, the α phase exhibited higher contrast between light and dark bands compared to the δ phase (Figure S2).[36] At a crystallization temperature of 130 °C, the pitch decreased 20-fold from 385 ± 20 μm to 20 ± 3 μm with increasing PVP MW of 10 kDa to 1300 kDa. Fig. 2E shows that the effect of MW on pitch was diminished at lower crystallization temperatures. Below 100 °C, the α phase was present in all samples, with pitches between 5 and 15 μm for all blend compositions (Figure S3).

### 2.2. Dynamic properties of melt-phase D-mannitol/PVP blends

Additives that encourage twisting are thought to suppress nucleation and promote the growth of crystals as thin fibrils with high aspect ratios and small torsional constants.[37,38] Considering that the total PVP concentration was constant at 15 wt%, the major difference in *P* across the samples must be related to the polymer chain dynamics in the melt, which depends strongly on the molecular weight. Small-amplitude oscillatory shear was used to quantify the dynamic properties of D-mannitol/PVP melts as a function of PVP molecular weight. Blends of D-mannitol and PVP powders of varied molecular weights were loaded into a rotational rheometer with a bob and cup geometry with diameters of 25 mm and 27 mm, respectively. The temperature was raised to 180 °C to melt the blend. After holding the sample at 180 °C for 5 min, the gap between the bottom of the cup and bob was reduced from 3 - 4 mm to 1 ± 0.3 mm. The temperature was then decreased to the desired setpoint for small-amplitude oscillatory shear (SAOS) experiments in

which the cup was oscillated clockwise and counter-clockwise at specified frequencies and strain amplitudes while the bob remained fixed.

Time sweep tests illustrated in Fig. 3A were conducted by oscillating the cup at a fixed strain amplitude of 50 % and frequency of 10 rad/s for D-mannitol melts with 15 wt% PVP of varied MWs. All compositions behaved as viscous fluids with $G'' > G'$, both of which increased with PVP MW. Longer polymer chains are more entangled thereby increasing viscosity and the elasticity of the blend.[39] For all four compositions, $G'$ and $G''$ were independent of time, indicating that the physicochemical properties of the blends did not change during oscillatory-shear deformation.[40,41].

The strain amplitude was varied from 10 % to 500 % at a fixed frequency of 100 rad/s, as displayed in Fig. 3B. Melts with PVP10 and PVP40 had constant complex moduli across the strain amplitude range. Based on the relatively low elasticity (small $G'$), it can be inferred that the blends approach Newtonian-like behavior at this temperature. For D-mannitol melts incorporating PVP360 and PVP1300, on the other hand, $G'$ and $G''$ were independent of frequency only below a strain amplitude of 40 %. Above this value, $G'$ and $G''$ decreased with increasing strain amplitude, a non-linear characteristic of non-Newtonian fluids[42,43] previously observed in PVP solutions.[44] At large applied strain amplitudes, shear forces can cause polymer chain disentanglement (reduction in entanglement density), resulting in a lower resistance to deformation and a decrease in $G'$ and $G''$.[45] Strain sweep tests were also carried out with low frequency at 1 rad/s (Figure S4) where all blends were in the linear region independent of PVP MW.

Frequency sweep tests in the range of 0.1 – 100 rad/s were performed at a fixed strain amplitude of 40 % where the dynamic properties were in the linear viscoelastic range regardless of the frequency while maximizing the torque for better signal to noise ratios. As displayed in Fig. 3C, $G'$ and $G''$ both increased monotonically with increasing frequency, with no apparent cross-over between $G'$ and $G''$ for all D-mannitol/PVP blends. The change in frequency is tantamount to changing the characteristic time for deformation so that the fingerprints of the linear viscoelastic behavior of the blends could be characterized over a broad range of Deborah numbers (relaxation times of the blend divided by the characteristic time for deformation). Elasticity becomes more pronounced with decreasing characteristic time for deformation (inverse of frequency). For the entire range of frequencies $G''\ll G'$, emphasizing the minor contribution that elasticity makes in comparison to viscous dissipation over a broad range of characteristic times.

The magnitude of complex viscosity, $|\eta^*|$, was extracted from the frequency-dependent behavior of $G'$ and $G''$ using the equation $|\eta^*| = \sqrt{(G'/\omega)^2 + (G''/\omega)^2}$. For all four blends, $|\eta^*|$ was frequency-independent at a strain amplitude of 40 %, a hallmark of behavior approaching that of Newtonian-like fluids. Fig. 3D summarizes $|\eta^*|$ values measured for D-mannitol melts incorporating 15 wt% PVP with varying molecular weights collected from 150 to 180 °C. Below 150 °C, the blends crystallized before their rheological properties could be characterized. For comparison, $|\eta^*|$ of pure D-mannitol melts was measured to be 0.02 Pa•s at 180 °C. The presence of 15 wt% PVP significantly increases $|\eta^*|$ even for PVP10.$|\eta^*|$ was found to increase with decreasing temperature, but we emphasize that $|\eta^*|$ could be varied at constant temperature by changing the MW of the PVP additive. Polymer chain mobility decreases with decreasing temperature, corresponding to increased resistance to deformation and larger $|\eta^*|$. Within the temperature range of 150 – 180 °C, $|\eta^*|$ varied within one order of magnitude for all blend compositions. Varying the PVP MW had a greater impact on $|\eta^*|$. At $T_c = 180$ °C, $|\eta^*|$ was measured to be 0.1 Pa•s

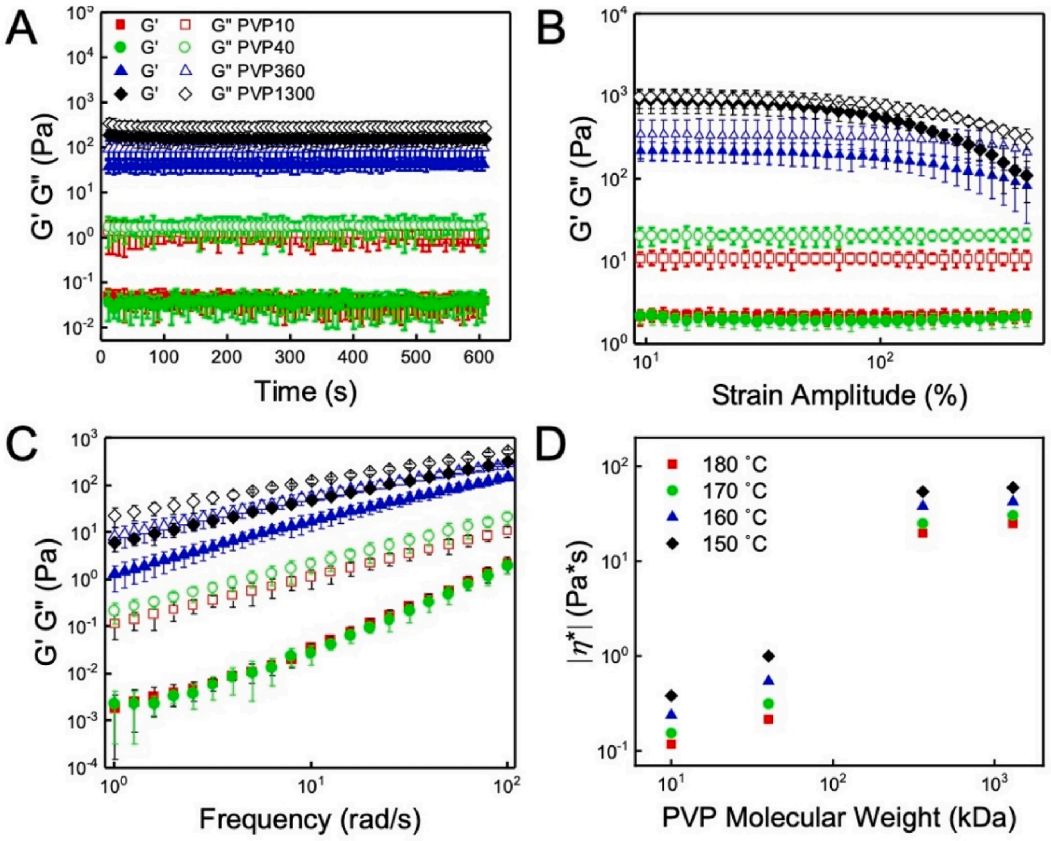


**Fig. 3.** Dynamic properties of D-mannitol melts incorporating 15 wt% PVP10, PVP40, PVP360 and PVP1300 at 180 °C. A) Time sweep test at 50 % strain amplitude and a frequency of 10 rad/s. B) Strain amplitude sweep test at a fixed frequency of 100 rad/s. C) Frequency sweep test at 40 % strain amplitude. D) $|\eta^*|$ versus PVP MW at temperatures ranging from 150 to 180 °C.

and 25 Pa•s for D-mannitol blends with 15 wt% PVP10 and PVP1300, respectively. This trend of increasing $|\eta^*|$ with increasing PVP MW is consistent with longer PVP chains exhibiting a greater density of entanglements that resist deformation compared to shorter PVP chains.

### 2.3. Pitch size dependence on $|\eta^*|$

Rheological characterization of D-mannitol/PVP blends showed $|\eta^*|$ varying over two orders of magnitude as a function of temperature and PVP MW. We next examined the relationship between $|\eta^*|$ and $P$ for D-mannitol/PVP blends crystallized as thin films from the melt. For temperatures below 150 °C in which the blends crystallized too quickly to be characterized via SAOS, we used an Arrhenius equation with the form $|\eta^*| = Ae^{\frac{-E_a}{RT}} + \eta_0$ to extrapolate $|\eta^*|$ at lower temperatures.[46,47] Here, $\eta_0$ is the D-mannitol viscosity at 180 °C. The preexponential factor is typically a function of polymer concentration or polymer MW. The values of $|\eta^*|$ obtained from SAOS for D-mannitol/PVP blends with different MWs were used as starting data for the extrapolation. In the lower temperature region, where D-mannitol blends crystallize fast, they cannot be considered as pure liquids since crystal nuclei significantly contribute to $|\eta^*|$. [48] For this reason, $|\eta^*|$ was used only to estimate the relationship between $P$ and $|\eta^*|$. We then re-plotted the data in Fig. 2 by replacing the crystallization temperature with $|\eta^*|$ on the x axis (Fig. 4). For all four blends, maximum twisting pitches of ~ 800–1000 μm were measured at smaller values of $|\eta^*|$ and minimum $P$ values of ~ 10 μm were measured at larger $|\eta^*|$. The $|\eta^*|$ values, at which these maximum and minimum $P$ values were observed, however, depended strongly on the PVP MW. $P = 5$ μm, for example, was observed for blends with 15 wt % PVP10 and $|\eta^*| = 5.1$ Pa·s and with 15 wt% PVP40 and $|\eta^*| = 1.1 \times 10^8$ Pa·s. In general, the pitch varied widely across $|\eta^*|$ values, indicating that $|\eta^*|$ is not the primary factor governing $P$.

There is not a direct relationship between the entanglement of PVP chains, the number of which significantly increases with MW, and the local environment in which D-mannitol crystallizes. Still, Fig. 2 demonstrates the existence of large differences of D-mannitol twisting for different PVP MWs, which may be related to the polymer chain time-dependent behavior in response to dynamic stresses. To test this idea, we next examined crystallization during the application of steady shear stresses.

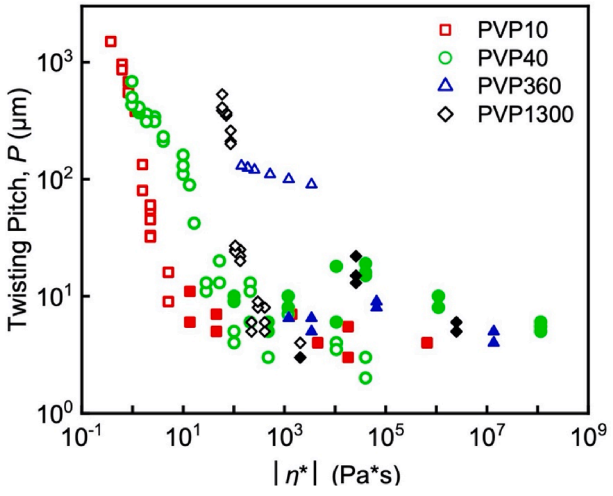


**Fig. 4.** Twisting pitch, $P$, versus $|\eta^*|$ for D-mannitol blends incorporating 15 wt % PVP with varying MW. Open and filled symbols represent the δ and α polymorph, respectively.

### 2.4. Crystallization of D-mannitol/PVP blends under steady shear

The melts were exposed to steady torsional shear between two parallel plates using a Linkam optical shearing stage. The bottom plate was rotated continuously in one direction while the top plate remained fixed. The twisting pitch, $P$, was measured at 7.5 mm from the center of the parallel plates. Steady torsional shear was applied to D-mannitol melts at shear rates ranging from 0 to 100 $s^{-1}$ for 30 s at 180 °C and was continuously applied as the sample was cooled at a rate of 30 °C/min and subsequently held at 130 °C until the film completely crystallized. Fig. 5A – C display POMs of D-mannitol films incorporating 15 wt% PVP1300, crystallized while exposed to steady torsional shear rates of 0, 1 and 100 $s^{-1}$, respectively. $P$ decreased with increasing shear rate. Fast Fourier transforms of the images, provided as insets in Fig. 5, were used to determine $P$, which decreased from 27 μm (no shearing) to 8 μm (high shear rate of 100 $s^{-1}$).

To test the role of polymer chain length on the shear rate dependence of $P$, we repeated these experiments using blends with 15 wt% PVP10 and small-molecule D-sorbitol, previously identified as an alternative twisting agent for D-mannitol.[30] Fig. 5D displays the dependence of $P$ on the apparent steady torsional shear rate in the range of 0.01 $s^{-1}$ to 100 $s^{-1}$ applied during film crystallization at 130 °C. For both blends incorporating 15 wt% PVP, $P$ decreased from 27 ± 5 μm at a shear rate of 0.01 $s^{-1}$ to 6 ± 2 μm at a shear rate of 100 $s^{-1}$, independent of the PVP MW. For 15 wt% D-sorbitol blends, on the other hand, $P$ remained at approximately 1500 – 2000 μm across all apparent shear rates tested (see Figure S5 for the corresponding POMs).

Shear stress has previously been identified to affect polymer chain conformations in solution, with polymer chains orienting and elongating along the shear direction.[49–53] D-Mannitol and PVP are miscible at high temperatures and can be considered as solutions where PVP and D-mannitol play the roles of solute and solvent, respectively.[48,54–56] During steady torsional shear, PVP chains are expected to disentangle and stretch in response to shear forces, which leads to increasing interactions between the PVP and D-mannitol. We hypothesize that the presence of PVP promotes D-mannitol crystallization as thin fibrils with a greater propensity to twist compared to thicker crystals. We do not expect shearing to affect D-mannitol itself, as $P$ for D-mannitol/D-sorbitol blends remains unchanged across a broad range of shear rates.

To the best of our knowledge, the role of applied shear forces on the crystal twisting pitch in small-molecule banded spherulites has not been previously reported, but several investigations touched this issue for banded spherulites of polymers and polymer blends. While no effect of shearing on the formation of banded spherulites was observed for injection-molded linear low density poly(ethylene)/high density poly (ethylene) blends,[57] shearing was required to induce banded spherulite formation in single-component high density poly(ethylene). [58–60] In the latter case, the presence of flow fields introduced during injection was hypothesized to create asymmetry in surface stresses at the crystallization front, resulting in the twisting of crystalline lamellae about the growth front.[58] Recently, shear-induced decrease in twisting pitch was observed in banded spherulites of poly(oxymethylene)/poly(butylene succinate) blends.[61] Shear forces were introduced by dragging a glass fiber through the polymer blend melt as it crystallized. The twisting pitch decreased linearly with shear rate from 23.3 μm under quiescent conditions to 11.5 μm at a shear rate of 320 $s^{-1}$. Interfacial shear stresses were thought to align molecular chains at the spherulitic growth front to initially form edge-on lamellae which then twisted upon further growth and branching. For D-mannitol/PVP blends examined here, the polymer is the minority phase and the exact mechanism of how its presence induces crystal twisting in D-mannitol is unknown. Nevertheless, our results are consistent with previous findings that shear-induced changes in polymer chain conformations can affect the twisting intensity in banded spherulites.

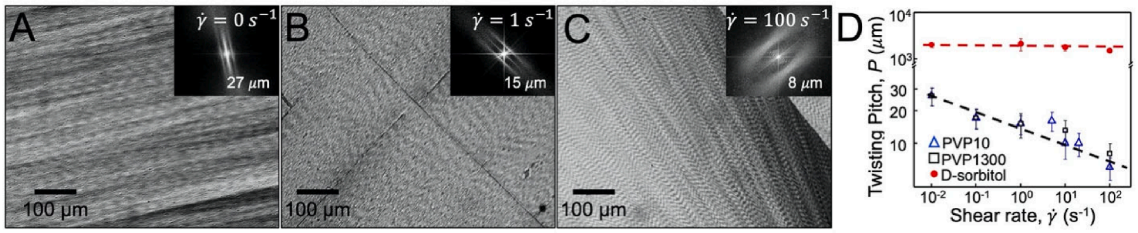


**Fig. 5.** A – C) POMs of D-mannitol films with 15 wt% PVP1300 crystallized at 130 °C while exposed to steady torsional shear at a rate of 0, 1, and 100 $s^{-1}$, respectively. Fast Fourier transforms of the images are provided as insets, with characteristic spacings corresponding to the twisting pitch extracted from the images also provided. D) Twisting pitch, *P*, versus steady torsional shear rate for D-mannitol films incorporating 15 wt% PVP10, PVP1300 and 15 wt% D-sorbitol crystallized at 130 °C.

### 2.5. Dependence of pitch on relaxation time

To understand the large dependence of *P* on PVP MW, we considered transient shear forces during melt processing. D-Mannitol crystallization occurred under quiescent conditions, but the melt was exposed to shear forces prior to crystallization. Specifically, powdered D-mannitol/PVP blends were melted between two glass slides at 180 °C and then the melt was compressed to decrease the film thickness, i.e. the compressive squeeze flow was applied.[62] This compressive force, applied over several seconds, introduced shear and extensional stresses as the melt flows in the radial direction in between the two glass slides. In response, PVP chains deform and elongate. Once flow stops and the compressive force is removed, the polymer chains can relax to their equilibrium conformation. As previously observed in other polymer blends, high MW PVP chains relax more slowly compared to low MW PVP chains.[63] We hypothesize that this difference in time-dependent behavior of PVP as a function of MW gives rise to significant differences in *P*.

To test our hypothesis, we varied the time between compressing the melt and cooling it to induce crystallization. Fig. 6A displays the time dependent temperature profile of a sample during such experiments. The hold time at 180 °C between compressing the melt and transferring the sample to the desired crystallization temperature was varied between 0 and 10 min. Fig. 6B displays the dependence of *P* on the hold time for D-mannitol blends incorporating 15 wt% PVP10 and PVP1300. D-Mannitol/PVP10 films exhibited average *P* values of ~ 350 μm for all hold times. In contrast, *P* increased from 25 μm to 150 μm as the hold time increased from 0 to 10 min for D-mannitol/PVP1300 films.

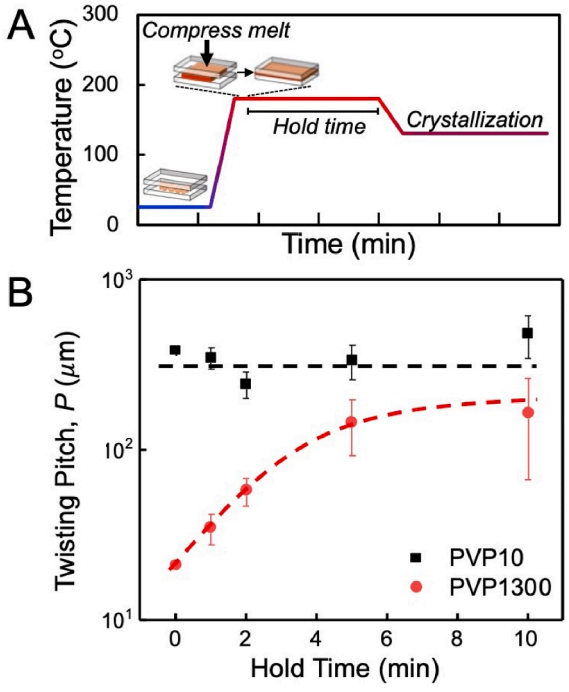


**Fig. 6.** A) Time-dependent temperature profile of the melting and crystallization of D-mannitol films. Melts were briefly compressed at 180 °C to decrease the film thickness, after which the samples were held at 180 °C for 0–10 min before cooling to the crystallization temperature. B) Twisting pitch, *P*, versus hold time for D-mannitol blends incorporating 15 wt% PVP10 and PVP1300 and crystallized at 130 °C. Dashed lines are provided to guide the eye.

The dependence of *P* on the hold time for D-mannitol/PVP1300 films but not D-mannitol/PVP10 films suggests the time-dependent polymer chain relaxation kinetics to be responsible for large pitch differences (Fig. 2). For short hold times, PVP1300 chains do not have time to relax to their equilibrium structure prior to crystallization. When the chains are provided sufficient time to relax, on the other hand, *P* becomes insensitive to the polymer chain length. This sensitivity to polymer chain conformation is most obvious at higher crystallization temperatures. At lower crystallization temperatures, the driving force for D-mannitol crystal twisting is very large and twisting may become less sensitive to the twist-inducing additive.

## 3. Conclusion

The incorporation of high viscosity additives is an established method of promoting twisting in crystals of small molecular compounds from the melt. Here, we employed comprehensive rheological characterization to measure the magnitude of complex viscosities and other linear viscoelastic material functions of D-mannitol melts in the presence of PVP with MWs ranging from 10 to 1300 kDa. Our results suggest that the mechanism of additive-induced crystal twisting is not related to the melt viscosity itself, but to local interactions between the additives and the crystals during crystallization. It has previously been established that the twisting sense, either clockwise or counterclockwise, can be determined by the chirality of a twist-inducing additive.[64] Here, we show that crystal twisting is also sensitive to the additive conformation. Twisting pitches of banded D-mannitol spherulites decreased when crystallization occurred under steady torsional shear, which likely induces the orientation and extension of polymer chains along the flow direction. Our findings also reveal the sensitivity of crystal twisting to processing conditions, in particular, to the amount of time provided for blends to equilibrate prior to crystallization. Looking forward, melt shearing under appropriate conditions may provide a way to control twisting pitches and e.g. reduce crystal twisting pitches below 1 μm to form iridescent films based on periodic variations in refractive indices.

## 4. Experimental methods

**Materials**. D-Mannitol and D-sorbitol were purchased from Sigma Aldrich (purity ≥ 98 %). Polyvinylpyrrolidone (PVP) powders with average molecular weights of 10 kDa, 40 kDa, 360 kDa and 1300 kDa were also purchased from Sigma-Aldrich. All materials were used without further purification.

**Film fabrication and characterization.** D-Mannitol was co-dissolved in water with the desired additive, either PVP or D-sorbitol, at a ratio of 85:15 wt% of D-mannitol to additive. Solutions were stirred for two hours before being transferred to a glass petri-dish and dried in a vacuum oven at 60 °C overnight. The dried mixture was collected and ground into a fine powder with a mortar and pestle. To form films, 1–2 mg of the powder was sandwiched between two glass slides. The sample was then transferred to a hot plate at 180 °C, which is above the melting point of D-mannitol ($T_m$ = 165 °C). Upon melting, a compressive force was applied to squeeze the melt into a 2–3 μm-thick film. The sample was then immediately transferred to the desired temperature and allowed to completely crystallize before cooling to room temperature. For relaxation experiments, the hold time between application of the compressive force and transfer of the sample to the crystallization temperature was varied from 0 to 10 min. Films were imaged between crossed polarizers to determine twisting pitches. Fast Fourier transforms of images were carried out using ImageJ.

**Grazing incidence wide-angle X-ray scattering (GIWAXS).** GIWAXS patterns on D-mannitol films were conducted at Beamline 11-BM at the Brookhaven National Laboratory National Synchrotron Light Source II. Diffraction patterns were collected with an incident X-ray wavelength of 0.9184 Å wavelength, a beam size of 0.2x0.05 mm and acquisition times of 10 s using a Pilatus800k detector at a sample-to-detector distance of 260 mm. Top cover slides were removed from the films prior to diffraction experiments.

**Small-amplitude oscillatory shear (SAOS) experiments.** Dynamic rheological testing was carried out via SAOS using a cup and bob geometry using an Advanced Rheometric Expansion System (ARES) rheometer from TA instruments, New Castle, DE. The strain ($\gamma$) was applied sinusoidally with respect to time ($t$), at a frequency $\omega$, i.e. $\gamma(t) = \gamma^0 \sin(\omega t)$, where $\gamma^0$ is the strain amplitude. The response shear stress $\tau(t)$, corresponding the oscillatory deformation, comprises two contributions, the energy stored as elastic energy ($G'(\omega)$) and the energy dissipated as heat ($G''(\omega)$), with $\tau(t) = G'(\omega)\gamma^0 sin(\omega t) + G''(\omega)\gamma^0 cos(\omega t)$. The magnitude of the complex viscosity $|\eta^*|$ was calculated using the equation, $|\eta^*| = \sqrt{(G'/\omega)^2 + (G''/\omega)^2}$.

**Crystallization under steady torsional flow.** Crystallization under steady torsional shear was carried out using a CSS450 Linkam shearing stage integrated with a Zeiss Axioskop 40 microscope. The observation window with a diameter of 2.8 mm sits at a fixed radial position 7.5 mm from the center. Shearing of D-mannitol/PVP and D-mannitol/D-sorbitol melts took place between two parallel quartz glass plates (55 mm diameter bottom and 32 mm diameter top) in which the bottom plate was rotated while the top plate remained fixed. 1–2 g of D-mannitol/PVP mixed powder was loaded onto the bottom plate. The gap between top and bottom plate was set to 1500 μm and the temperature raised to 180 °C at a rate of 30 °C/min. After reaching 180 °C, the sample was held at this temperature for two minutes to completely melt the powder. The gap between the two plates was then decreased at a rate of 500 μm/min to 5 μm. Steady torsional shear was applied during the cooling process and was continuously applied at the crystallization temperature until crystallization was complete.

**Conflicts of interest**.

There are no conflicts to declare.

*CRediT authorship contribution statement*

**Yuze Zhang:** Methodology, Investigation, Validation, Writing – original draft. **Alexander G. Shtukenberg:** Methodology, Supervision, Writing – review & editing. **Bart Kahr:** Supervision, Writing – review & editing, Resources, Funding acquisition. **Dilhan M. Kalyon:** Supervision, Methodology, Writing – review & editing. **Stephanie S. Lee:** Conceptualization, Supervision, Resources, Project administration, Funding acquisition.

## Declaration of Competing Interest

The authors declare that they have no known competing financial interests or personal relationships that could have appeared to influence the work reported in this paper.

## Data availability

Data will be made available on request.

## Acknowledgements

This work was primarily supported by the National Science Foundation DMR-2003997 and secondarily by the New York University Materials Research Science and Engineering Centre (MRSEC) program of the National Science Foundation under award number DMR-1420073. The research used the Complex Materials Scattering (CMS) beamline of the National Synchrotron Light Source II (NSLS-II), which is an U.S. DOE Office of Science Facility, at Brookhaven National Laboratory under Contract No. DE-SC0012704, and we thank Dr. Ruipeng Li and Dr. Masafumi Fukuto for help with GIWAXS experiments. The authors also acknowledge support from PSEG Foundation to advance energy innovation at Stevens Institute of Technology.

## References

[1] A.G. Shtukenberg, X. Zhu, Y. Yang, B. Kahr, Cryst. Growth Des. 20 (2020) 6186–6197.
[2] J. Xu, H. Ye, S. Zhang, B. Guo, Crystals 7 (2017) 241.
[3] C.Y. Li, S.Z.D. Cheng, J.J. Ge, F. Bai, J.Z. Zhang, I.K. Mann, F.W. Harris, L.-C. Chien, D. Yan, T. He, B. Lotz, Phys. Rev. Lett. 83 (1999) 4558–4561.
[4] A.J. Lovinger, Macromolecules 53 (2020) 741–745.
[5] Y. Li, H. Huang, Z. Wang, T. He, Macromolecules 47 (2014) 1783–1792.
[6] Y. Li, H. Huang, T. He, Z. Wang, ACS Macro Lett. 1 (2012) 154–158.
[7] B. Crist, J.M. Schultz, Prog. Polym. Sci. 56 (2016) 1–63.
[8] M.R. Kamal, D.M. Kalyon, J.M. Dealy, Polym. Eng. Sci. 20 (1980) 1117–1125.
[9] J. Yang, C.T. Hu, A.G. Shtukenberg, Q. Yin, B. Kahr, CrystEngComm 20 (2018) 1383–1389.
[10] Y. Yang, Y. Zhang, C.T. Hu, M. Sun, S. Jeong, S.S. Lee, A.G. Shtukenberg, B. Kahr, Chem. Mater. 34 (2022) 1778–1788.
[11] M.M. Degen, N. Costanzino, J. Bechhoefer, J. Cryst. Growth 209 (2000) 953–962.
[12] B. Sadlik, L. Talon, S. Kawka, R. Woods, J. Bechhoefer, Phys. Rev. E 71 (2005), 061602.
[13] L. Ye, J. Qiu, T. Wu, X. Shi, Y. Li, RSC Adv. 4 (2014) 43351–43356.
[14] H. Tanaka, T. Hayashi, T. Nishi, J. Appl. Phys. 59 (1986) 3627–3643.
[15] K. Wang, L. Cai, S. Jesse, S. Wang, Langmuir 28 (2012) 4382–4395.
[16] H.-M. Ye, J. Xu, J. Freudenthal, B. Kahr, J. Am. Chem. Soc. 133 (2011) 13848–13851.
[17] X. Cui, A.G. Shtukenberg, J. Freudenthal, S. Nichols, B. Kahr, J. Am. Chem. Soc. 136 (2014) 5481–5490.
[18] Y. Yang, K. Zong, S.J. Whittaker, Z. An, M. Tan, H. Zhou, A.G. Shtukenberg, B. Kahr, S.S. Lee, Mol. Syst. Des. Eng. 7 (2022) 569–576.
[19] D. Patel, D.C. Bassett, Proc. R. Soc. Lond. A 445 (1994) 577–595.
[20] B. Lotz, S.Z.D. Cheng, Polymer 46 (2005) 577–610.
[21] D.C. Bassett, Polymer 47 (2006) 3263–3266.
[22] H.-M. Ye, J.-S. Wang, S. Tang, J. Xu, X.-Q. Feng, B.-H. Guo, X.-M. Xie, J.-J. Zhou, L. Li, Q. Wu, G.-Q. Chen, Macromolecules 43 (2010) 5762–5770.
[23] H.D. Keith, F.J. Padden, Macromolecules 29 (1996) 7776–7786.
[24] Y.O. Punin, O.I. Artamonova, Crystallogr. Rep. 46 (2001) 138–143.
[25] A.G. Shtukenberg, J. Freudenthal, B. Kahr, J. Am. Chem. Soc. 132 (2010) 9341–9349.
[26] B. Kahr, A. Shtukenberg, E. Gunn, D.J. Carter, A.L. Rohl, Cryst. Growth Des. 11 (2011) 2070–2073.
[27] Y.O. Punin, A.G. Shtukenberg, Autodeformation Defects in Crystals, St. Petersburg Univ. Press, St. Petersburg, 2008.
[28] W.A. Tiller, The Science of Crystallization: Microscopic Interfacial Phenomena, Cambridge University Press, Cambridge, 1991.
[29] B. Sadlik, Master of Science, Simon Fraser University, 2004.
[30] A.G. Shtukenberg, X. Cui, J. Freudenthal, E. Gunn, E. Camp, B. Kahr, J. Am. Chem. Soc. 134 (2012) 6354–6364.
[31] X. Cui, A.L. Rohl, A. Shtukenberg, B. Kahr, J. Am. Chem. Soc. 135 (2013) 3395–3398.
[32] A.G. Shtukenberg, A. Gujral, E. Rosseeva, X. Cui, B. Kahr, CrystEngComm 17 (2015) 8817–8824.
[33] B.F.S. Safitri, E.M. Woo, Crystals 12 (2022) 807.
[34] T.-Y. Chen, E.M. Woo, S. Nagarajan, Sci. Rep. 10 (2020) 4062.
[35] F.R. Fronczek, H.N. Kamel, M. Slattery, Acta Crystallogr. C 59 (2003) o567–o570.

[36] X. Cui, S.M. Nichols, O. Arteaga, J. Freudenthal, F. Paula, A.G. Shtukenberg, B. Kahr, J. Am. Chem. Soc. 138 (2016) 12211–12218.
[37] L. Yu, J. Am. Chem. Soc. 125 (2003) 6380–6381.
[38] J. Tao, L. Yu, J. Phys. Chem. B 110 (2006) 7098–7101.
[39] W.M. Kulicke, R. Kniewske, Rheol. Acta 23 (1984) 75–83.
[40] J.A. Lee, M. Kontopoulou, J.S. Parent, Polymer 45 (2004) 6595–6600.
[41] D.S. Kalika, D.W. Giles, M.M. Denn, J. Rheol. 34 (1990) 139–154.
[42] A.J. Poslinski, M.E. Ryan, R.K. Gupta, S.G. Seshadri, F.J. Frechette, J. Rheol. 32 (1988) 703–735.
[43] A. Vázquez-Quesada, R.I. Tanner, M. Ellero, Phys. Rev. Lett. 117 (2016), 108001.
[44] D. Xu, C.-Y. Liu, S.L. Craig, Macromolecules 44 (2011) 2343–2353.
[45] J.F. Ryder, J.M. Yeomans, J. Chem. Phys. 125 (2006), 194906.
[46] C.T. Moynihan, S. Cantor, J. Chem. Phys. 48 (1968) 115–119.
[47] S. Sathivel, J. Huang, W. Prinyawiwatkul, J. Food Eng. 84 (2008) 187–193.
[48] K. Kobayashi, T. Nagasawa, J. Macromol. Sci. B 4 (1970) 331–345.
[49] A. Link, J. Springer, Macromolecules 26 (1993) 464–471.
[50] C.-C. Huang, R.G. Winkler, G. Sutmann, G. Gompper, Macromolecules 43 (2010) 10107–10116.
[51] E.C. Lee, M.J. Solomon, S.J. Muller, Macromolecules 30 (1997) 7313–7321.
[52] K. Migler, C.-H. Liu, D.J. Pine, Macromolecules 29 (1996) 1422–1432.
[53] R. Gangopadhyay, J. Polym. Sci., Part B: Polym. Phys. 46 (2008) 2443–2455.
[54] J. Tao, Y. Sun, G.G.Z. Zhang, L. Yu, Pharm. Res. 26 (2009) 855–864.
[55] R.R. Lagasse, B. Maxwell, Polym. Eng. Sci. 16 (1976) 189–199.
[56] G. Kumaraswamy, J. Macromol. Sci. C 45 (2005) 375–397.
[57] B. Wang, H.-X. Huang, Polym. Eng. Sci. 52 (2012) 117–124.
[58] L. Huang, W. Yang, B. Yang, M. Yang, G. Zheng, H. An, Polymer 49 (2008) 4051–4056.
[59] K. Zhang, Z. Liu, B. Yang, W. Yang, Y. Lu, L. Wang, N. Sun, M. Yang, Polymer 52 (2011) 3871–3878.
[60] X. Liu, Y. Pan, C. Peng, X. Hao, G. Zheng, D.W. Schubert, C. Liu, C. Shen, Mater. Lett. 172 (2016) 19–22.
[61] W.-J. Sun, W. Liu, Y. Ren, X. Miao, L. Xu, G.-J. Zhong, J. Lei, F. Bian, J.-Z. Xu, Z.-M. Li, ACS Appl. Polym. Mater. 1 (2019) 2741–2750.
[62] D.M. Kalyon, H.S. Tang, J. Nonnewton. Fluid Mech. 143 (2007) 133–140.
[63] T. Pakula, S. Geyler, T. Edling, D. Boese, Rheol. Acta 35 (1996) 631–644.
[64] H.-M. Ye, J.H. Freudenthal, M. Tan, J. Yang, B. Kahr, Macromolecules 52 (2019) 8514–8520.